Polymer Micelles as Supports for the Production of Millimetric Polyethylene Beads

Cécile Bouilhac,[†,‡] Eric Cloutet,[†,‡] Daniel Taton,[†,‡] Alain Deffieux,[†,‡] Redouane Borsali,[§] and Henri Cramail*[,†,‡]

Université de Bordeaux, Laboratoire de Chimie des Polymères Organiques, ENSCPB, 16 Avenue Pey-Berland, Pessac Cedex F33607, France, CNRS, Laboratoire de Chimie des Polymères Organiques, Pessac Cedex F33607, France, and CNRS, CERMAV, Grenoble Cedex F38041, France

Received July 24, 2008; Revised Manuscript Received September 3, 2008

ABSTRACT: The self-assembly in toluene of linear polystyrene functionalized in α-position by benzoic acid moieties into active micelle-like structures was exploited to trap trimethylaluminium and thus generate encapsulated methylaluminoxane-like species. These nanomicellar reactors were subsequently used as such or in the presence of free benzoic acid for supporting the tridentate bis(imino)pyridinyl iron catalyst for ethylene polymerization. In this way, high catalytic activities and polyethylenes (PEs) with unimodal chain distribution and controlled morphology were obtained. Remarkably well-defined spherical PE beads with an average diameter of 2 mm were produced when free benzoic acid was added to the micellar polymeric supports.

Introduction

Although metallocenes and late transition metal soluble complexes have proved to be effective in olefin polymerization catalysis, their heterogenization is required to control polymer morphology and prevent reactor fouling in industry. The main supports used to date are porous inorganic oxides, particularly silica.[1,2] As traces of these inorganic supports remain in the final polyolefins thus affecting the mechanical and optical properties of the final materials,[1,3] growing attention is currently paid to the development of purely organic—mainly polystyrene (PS)-based—supports.[4] The latter supports can be easily functionalized to fix the catalyst through its ligands[5−8] or can only serve for its encapsulation.[9,10] Alternatively, PS particles functionalized with poly(ethylene oxide)[11] or poly(propylene oxide)[12,13] chains on their surface were used to anchor methylaluminoxane (MAO)/metallocene complexes through oxygen−aluminum interactions. We have also recently shown that star-like PS composed of a nanogel core and PS arms carrying a small number of peripheral ethylene oxide units can serve as highly effective supports.[14] However, the multistep synthesis of the star-like PS and the use of high amounts of MAO as the main activator (MAO/metal > few thousands) for complete catalyst activation are limitations for an industrial development of such organic supports.

Following a different strategy, Borealis company has described a solidification process of metallocene/MAO solutions upon addition to perfluoroctane in order to obtain polymer particles.[15,16] A similar route has been followed by Klapper et al. who utilized emulsified MAO-activated metallocenes into a hydrocarbon/perfluorocarbon mixture.[17,18] Well-defined polyethylene and polypropylene nanoparticles, with high molar masses, were obtained in these conditions. In these approaches, although single-site polymerization catalysts free from an inert carrier are used, the presence of a further cosolvent is required. Following different strategies, Mecking et al. have also prepared aqueous dispersions of high molar mass polyethylene nanoparticles by microemulsion polymerization in the presence of nickel-based catalysts.[19−21]

Another important challenge is to find new activators as substitutes of MAO for metallocene and postmetallocene catalysts.[22,23] In this respect, aluminum alkoxides formed by reaction between benzophenone (BZ) or benzoic acid (BA) with trimethylaluminum (TMA) are known to readily activate iron based-complexes toward ethylene polymerization.[24,25] Heterogenization of these MAO-substitutes has been achieved by employing star-like PS supports bearing either one BZ or one BA unit at the periphery of their branches.[26,27] In a recent addition, we have demonstrated that spherical micellar objects obtained by the self-assembly in toluene of PS-*block*-poly(4-vinyl benzoic acid) block copolymers (PS-*b*-P(4-VBA)) can also be advantageously used as supports of iron-based complexes for the production of PE beads.[28] In this case, both MAO-like species generated from TMA and BA moieties and the iron-based complex are embedded within the micelles, the latter nanoreactors thus serving as efficient supports for the production of PE beads of micrometric size.

Following this strategy, we investigate in this work the use of micelle-like structures obtained by self-assembly in toluene of linear PS oligomers functionalized in α-position with a single BA unit (α-BA-PS) as organic supports of the tridentate bis(imino)pyridinyliron/TMA catalytic system. The latter supports can either be directly used as such or can be swelled with additional free benzoic acid molecules before embedding the catalytic system. The so-formed nanoreactors were then effectively used for the production of PE beads with a controlled morphology.

Experimental Section

Materials. All reagents were purchased from Aldrich. Toluene was purified by distillation over polystyryllithium. Styrene was stirred overnight over CaH_2 and distilled prior to use. TMA (2 M solution in heptane) was used as received. 2,6-Bis{1−2,6-(diisopropylphenyl)imino]ethylpyridynyl iron dichloride [MeDIP(2,6-iPrPh)$_2$FeCl$_2$] was synthesized as reported in the literature[29] and kept in a glovebox under argon atmosphere. Other reagents were used without further purification.

Synthesis of Benzoic Acid End-Functionalized PS by Atom Transfer Radical Polymerization. A dry round-bottom flask equipped with a magnetic stir bar was charged with 4-(1-bromoethyl)benzoic acid (0.47 g; 2.05 mmol), CuBr (0.29 g; 2.05 mmol), 2,2′ bipyridyl (bpy) (1.28 g; 8.2 mmol), and styrene (29.3 mL; 256 mmol). The flask was degassed by three freeze−pump−thaw

* Corresponding author. E-mail: cramail@enscpb.fr.
† Université de Bordeaux.
‡ CNRS, Laboratoire de Chimie des Polymères Organiques.
§ CNRS, CERMAV.

10.1021/ma8016772 CCC: $40.75
Published on Web 10/03/2008

Scheme 1. Synthesis of Benzoic Acid End-Functionalized Polystyrenes by ATRP and Elimination of the Bromine Atom

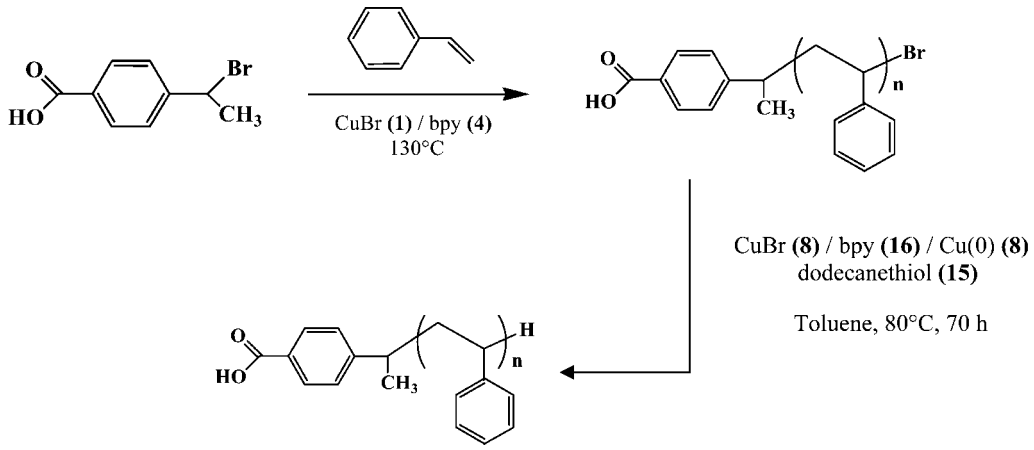

cycles and was immersed in an oil bath thermostatted at 130 °C for 50 min. The reaction mixture was filtered through SiO_2 to remove the catalyst using THF as the eluent. The polymer was precipitated into an excess of methanol and dried under vacuum. M_n = 3600 g/mol, M_w/M_n =1.10. ^{1}H NMR (400 MHz, $CDCl_3$): δ (ppm) = 0.99 (b, H^3), 2.37−1.40 (m, H^4, H^5), 4.48 (b, H^6), 7.10−6.40 (m, phenyl, H^2), 8−7.9 (b, aromatic of benzoic acid, H^1)

Elimination of the Bromo End Groups of the Benzoic Acid End-Functionalized PS. A dry round-bottom flask equipped with a magnetic stir bar was charged with the benzoic acid end-functionalized polystyrene (1.4 g; 0.39 mmol), CuBr (0.45 g; 3.12 mmol), bpy (0.97 g; 6.24 mmol), Cu^0 (0.20 g, 3.12 mmol), toluene (12.2 mL), and 1-dodecanethiol (1.4 mL; 5.85 mmol). The flask was degassed by three freeze−pump−thaw cycles and was immersed in an oil bath thermostatted at 80 °C for 70 h. The reaction mixture was filtered through neutral alumina to remove the catalyst using THF as the eluent. The polymer was precipitated into an excess of ethanol and dried under vacuum.

Typical Reaction between TMA and Benzoic Acid End-Functionalized PS. In a Schlenk tube equipped with a magnetic stirrer, 0.22 g (0.061 mmol) of benzoic acid end-functionalized PS (which can be associated with, for example, 0.61 mmol of "free" benzoic acid molecules) were introduced under argon atmosphere and freeze-dried. Dry toluene (12 mL) was then added, and the mixture was stirred for complete dissolution of the support. The desired amount of TMA was added dropwise at 0 °C using an ice bath. The Schlenk was then immersed in an oil bath thermostatted at 60 °C for 48 h.

Polymerization of Ethylene by the Fe Supported Catalyst. Dry toluene was added to the previous solution (V_{total} (toluene) = 40 mL), and the reaction mixture was connected to a 1 atm ethylene gas outlet using a rubber tube. Ethylene was bubbled through the Schlenk tube for 20 minutes to remove argon. Polymerization was initiated at 30 °C by adding the required amount of iron catalyst in toluene via a syringe. After 1 h of polymerization, the vessel was disconnected from the ethylene outlet, and the polymer was precipitated by adding methanol containing 2% HCl. The precipitated polymer was filtered, washed, and dried to constant weight.

Analysis. ^{1}H NMR spectra were recorded using Bruker AC-400 NMR spectrometer using $CDCl_3$ or toluene-d_8 at room temperature. Size exclusion chromatography (SEC) was performed in tetrahydrofuran at 25 °C at a flow rate of 1 mL/min using a refractometer (Varian) and a UV−visible spectrophotometer (Varian) operating at 254 nm and 4 TSK columns (G5000HXL (9 μm), G4000HXL (6 μm), G3000HXL (6 μm), and G2000HXL (5 μm)). Calibration was performed using linear polystyrene standards. The PE weight-average molar mass (M_w) and molar mass distribution were determined using a Waters GPCV2000 SEC instrument, equipped with one PLgel Olexis Guard (50 × 7.5 mm) column, three PLgel Olexis (300 × 7.5 mm) columns, and an online viscometer and refractive index detector, at 140 °C in 1,2,4-trichlorobenzene as solvent at a flow rate of 1 mL/min. Polyethylene beads were observed under transmission electron microscopy (TEM) performed on a HITACHI H7650 microscope operating at 100 kV. For observation of the interior of the PE beads, cryo-ultrathin sections were previously cut with an ultramicrotome Leica UltraCut UCT equipped with a cryo-chamber Leica EM FCS, and samples were chemically stained in RuO_4 vapor for 24 h. Scanning electronic microscopy (SEM) analyses were carried out on a JEOL JSM 2500 apparatus.

Dynamic light scattering (DLS) measurements were performed using an ALV laser goniometer, which consists of a 22 mW HeNe linear polarized laser with 632.8 nm wavelength and an ALV-5000/EPP multiple tau digital correlator with 125 ns initial sampling time. The samples were kept at constant temperature (25 °C) during all the experiments. The accessible scattering angle range is from 10° up to 150°. However, due to difficulties in removing dust, most of the dynamic measurements were done at diffusion angles higher than 40°. The solutions were introduced into 10 mm diameter glass cells. Dynamic light scattering measurements were evaluated by fitting of the measured normalized time autocorrelation function of the scattered light intensity. The data were fitted with the help of the constrained regularization algorithm (CONTIN),[30] which provides the distribution of relaxation times τ, $A(\tau)$, as the inverse Laplace transform of $g^{(1)}(t)$ function:

$$g^{(1)}(t) = \int_0^\infty A(\tau) \exp(-t/\tau)\, d\tau \qquad (1)$$

The apparent diffusion coefficient D was obtained by plotting the relaxation frequency, Γ ($\Gamma = \tau^{-1}$) versus q^2 where q is the wavevector defined as

Table 1. Synthesis by ATRP of Benzoic Acid End-Functionalized Polystyrenes[a,b]

initiator (I)	[M]/[I][c]	t (min)	$\bar{}M_{n,theo}$(100% conv)[d] (g/mol)	$\bar{\bar{}}M_{n,SEC}$[e] (g/mol)	$\bar{\bar{}}M_w/\bar{}M_n$ [e]	conversion (%)	$\bar{\bar{}}M_{n,NMR}$[f] (g/mol)
4-(1-bromoethyl)benzoic acid	125	50	13000	3600	1.1	28	3800
	125	80	13000	5200	1.1	40	5200
	125	85	13000	6100	1.1	47	6000

[a] Polymerization in bulk at 130 °C using 4-(1-bromoethyl) benzoic acid /CuBr/bpy = 1/1/4 [bpy = bipirydyl]. [b] Conditions for elimination of the bromine atom: α-BA-PS-Br/CuBr/bpy/Cu(0)/dodecanethiol = 1/8/16/8/15 at 80 °C for 70 h. [c] M = styrene and I = 4-(1-bromoethyl) benzoic acid. [d] $\bar{\bar{}}M_{n,theo}$ = (% conv × [M]/[I] × $M_{styrene}$) + $M_{initiator}$ (g/mol). [e] Determined by SEC with THF as eluent (RI detector). [f] Determined by ^{1}H NMR.

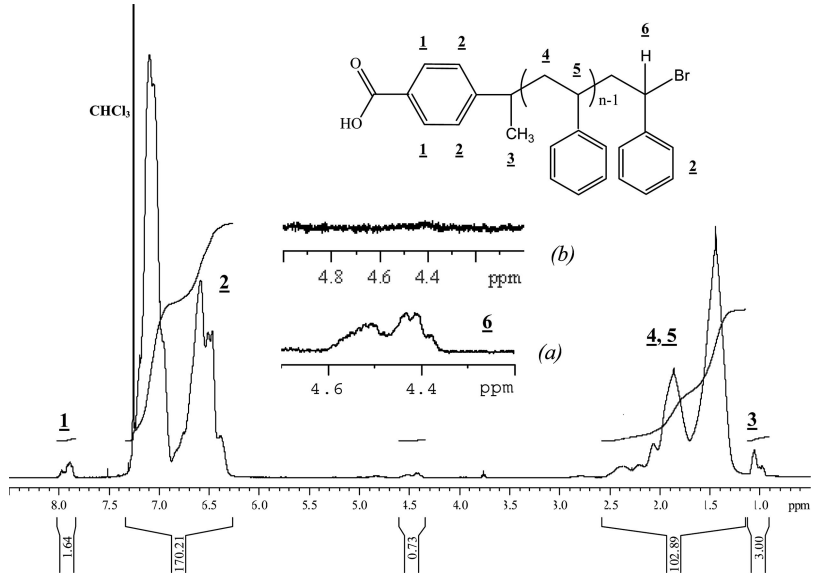

Figure 1. ^{1}H NMR spectra (400 MHz, $CDCl_3$) of benzoic acid end-functionalized polystyrene using CuBr/bpy as catalyst and 4-(1-bromoethyl) benzoic acid as initiator. Enlarged signal of the bromine α-proton before (a) and after (b) bromine elimination.

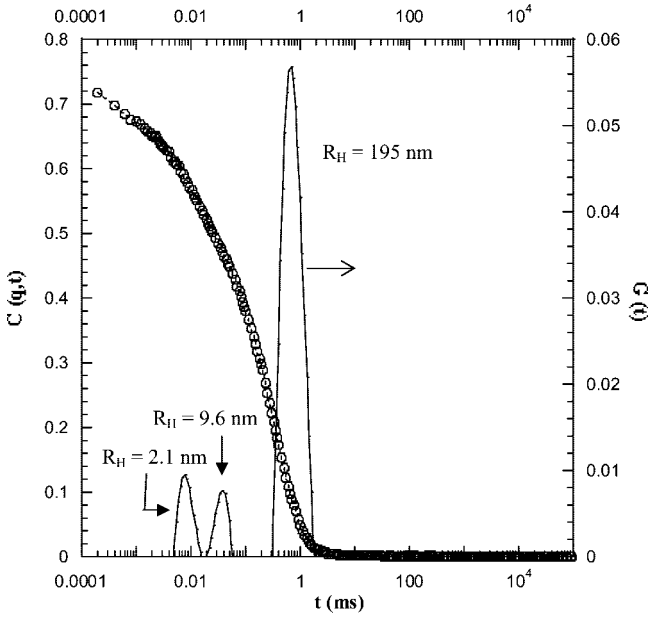

Figure 2. Autocorrelation function and relaxation times at $\theta = 90°$ of α-BA-PS ($M_n = 3600$ g/mol) in toluene ($c = 18$ mg/mL, $T = 25$ °C).

$$q = \frac{4\pi n}{\lambda} \sin\left(\frac{\theta}{2}\right) \tag{2}$$

and λ is the wavelength of the incident laser beam (632.8 nm), θ is the scattering angle, and n the refractive index of the media. The diffusion coefficient was then determined by extrapolation to zero concentration, and hydrodynamic radius (R_H) was calculated from the Stokes−Einstein relation

$$R_H = \frac{k_B T}{6\pi\eta\Gamma} q^2 = \frac{k_B T}{6\pi\eta D_{real}} \tag{3}$$

where k_B is the Boltzmann constant, Γ the relaxation frequency, T is the temperature, and η is the viscosity of the medium.

Solutions used for light scattering were prepared using the following method: toluene used as solvent was preliminarily filtered through a 0.22 μm PTFE membrane and added to polymer chains. The solutions were then left under stirring for 6 h at 25 °C for complete dissolution. All solutions were filtrated with 1 μm filters before analysis.

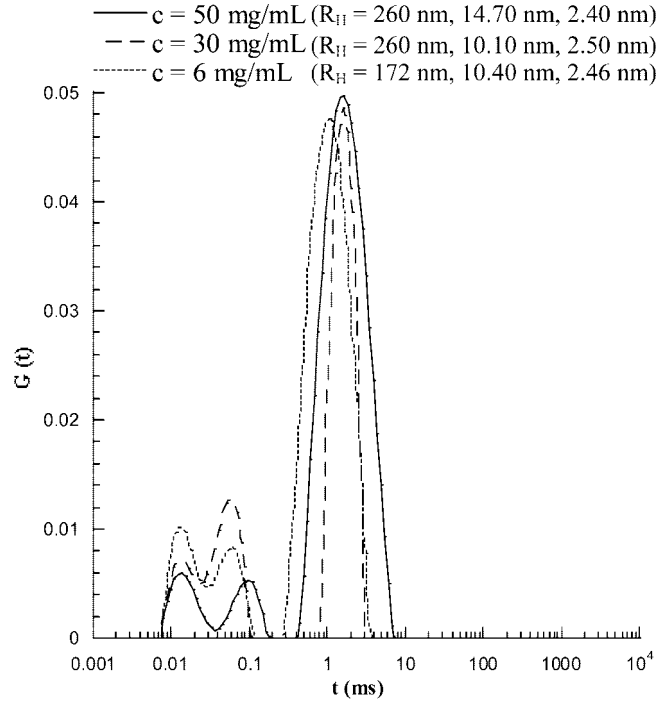

Figure 3. Relaxation times of α-BA-PS ($M_n = 5200$ g/mol and $\theta = 90°$) solutions prepared by direct polymer dissolution in toluene at different concentrations.

Results and Discussion

Synthesis of Benzoic Acid End-Functionalized Polystyrene. Linear polystyrenes (PS) bearing one benzoic acid and bromo end-groups in α- and in ω-positions, respectively (α-BA-PS-Br), were synthesized by atom transfer radical polymerization (ATRP) in bulk, using 4-(1-bromoethyl)benzoic acid as initiator and CuBr/bipyridyl (bpy) (1/4) as a catalytic system, following an already published procedure (see Scheme 1).[31,32] Polymerizations were stopped at monomer conversion of <50% so as to obtain α-BA-PS with a narrow molar mass distribution. Under these conditions, good control over the molar masses,

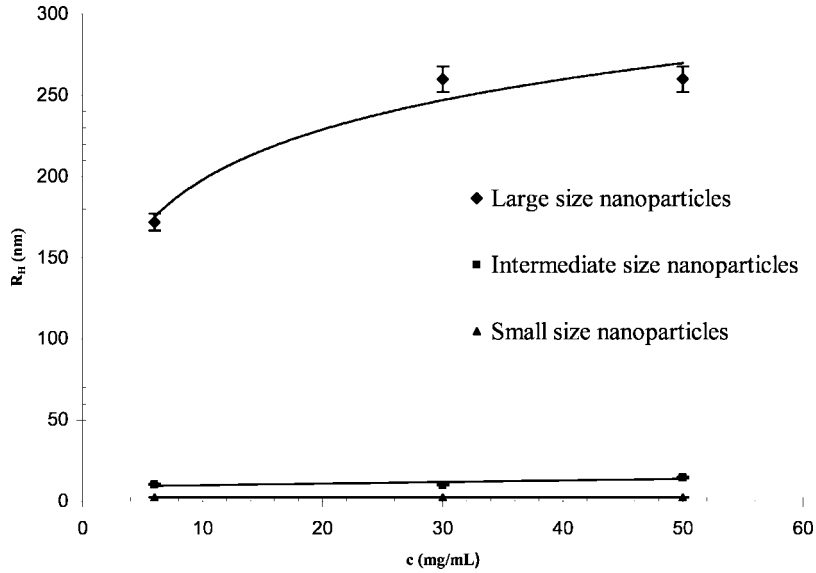

Figure 4. Hydrodynamic radii of nanoparticles with respect to [α-BA-PS] in toluene at 25 °C.

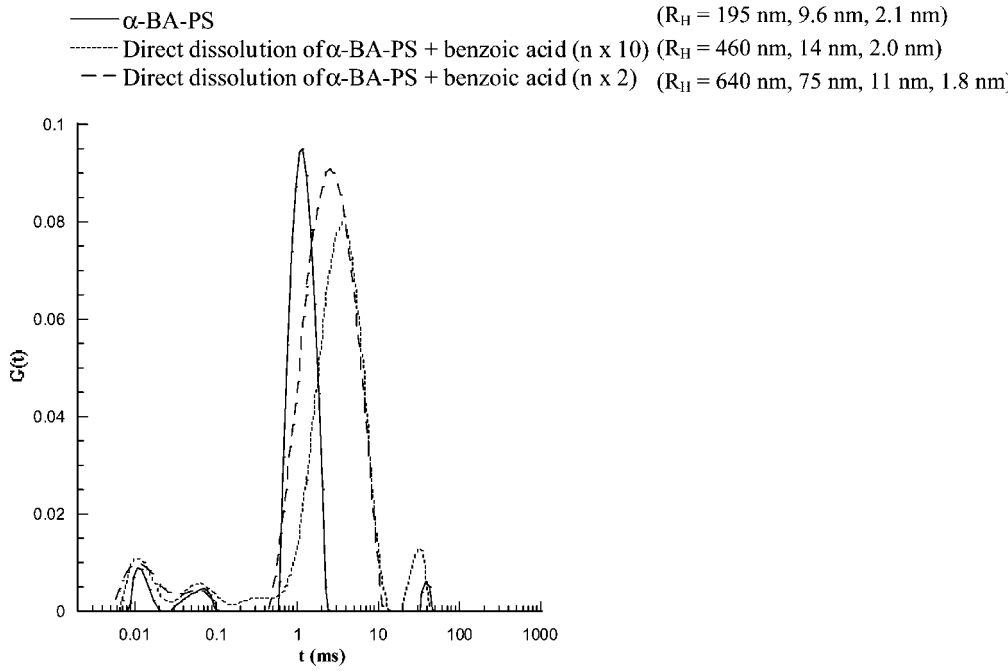

Figure 5. Relaxation times of toluene solutions of α-BA-PS (M_n = 3600 g/mol) at 18 mg/mL, in the presence and in the absence of BA molecules, at 25 °C (θ = 90°).

polydispersities, and functionalities could be achieved, as illustrated in Table 1. As can be seen, experimental M_n values determined by SEC and ^{1}H NMR assuming one benzoic acid group per PS chain are in good accordance.

Next was the removal of the ω-bromo end groups of the α-BA-PS-Br precursors. In our previous studies, indeed, we have verified that the presence of bromine termini of α-BA-PS-Br prevents ethylene polymerization. The substitution of the bromo function for a hydrogen atom was accomplished by chemical treatment of α-BA-PS-Br in the presence of dodecanethiol and Cu(0)/Cu(I) complexes (Scheme 1), yielding α-BA-PS-H.[26,27]

The presence of benzoic acid chain ends as well as the quantitative elimination of the bromine atoms were confirmed by ^{1}H NMR spectroscopy, as shown in Figure 1 (see inserts). The signals observed from 7.8 to 8 ppm are representative of the aromatic protons in α-position of the carboxyl group of BA, whereas the peak at 4.5 ppm corresponds to the proton located at the α-position of the bromine chain-end.

Solution Properties of α-BA-PS in Toluene by Dynamic Light Scattering. Dynamic light scattering (DLS) experiments were performed on α-BA-PS toluene solutions. Data revealed the existence of three relaxation times, corresponding to different size distributions, as shown in Figure 2. Due to the amphiphilic nature of α-BA-PS, the results suggest the existence of a self-assembly in toluene of α-BA-PS into micelles that likely consists of a BA core and a PS corona (toluene being a good solvent for PS[33,34] and a poor for BA (see Supporting Information section 2). The values of the hydrodynamic radii (R_H) of the different nanoparticles were calculated from the decay times using the Stokes−Einstein equation. These relaxation times were deduced from the CONTIN analysis[30] of the DLS correlation function and, as an example, are illustrated in Figure 2 for α-BA-PS (M_n = 3600 g/mol) at 18 mg/mL.

Scheme 2. Micellization of α-BA-PS in Toluene in the Absence or in the Presence of Free BA

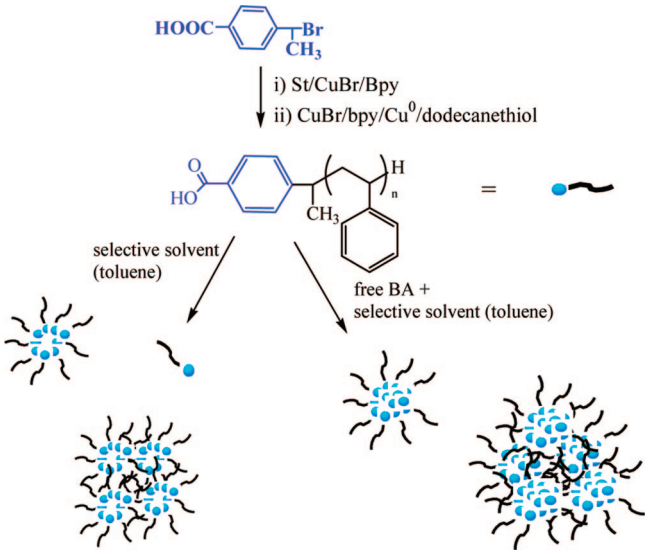

DLS experiments at various α-BA-PS concentrations allowed us to have a better insight of the three different nanoparticles (see Figure 3). Comparable results were obtained with the three polymers, hence, the main data presented here are those obtained from α-BA-PS with M_n = 5200 g/mol.

At the highest concentrations (30 and 50 mg/mL), DLS analyses show the presence of three main size distributions with R_H values corresponding to 2.50, 10.10, and 260 nm (±2.5%) and 2.40, 14.70, and 260 nm (±2.5%), respectively. At 6 mg/mL, the three size distributions are still observed but the size of the larger nanoparticles decreases to 172 nm. The evolution of the different hydrodynamic radii versus the concentration of α-BA-PS is illustrated in Figure 4.

One can note that the average size of the two smaller distributions do not or slightly vary with the α-BA-PS concentration in contrast to the larger one. Consequently, the two distributions of smaller size ($R_H \sim$ 2.5 and 10.0 nm) can be logically assigned, respectively, to α-BA-PS single chains (unimers) and to micellar structures formed by self-assembly. The third size distribution can be attributed to aggregates of micelles whose size increases with the concentration of α-BA-PS. A similar behavior was observed with the two other α-BA-PS samples of different molar mass. It is also important to mention that preparation of α-BA-PS solutions by dilution of a 'stock' polymer solution (initial concentration of 50 mg/mL) gives similar results in terms of micellar organization and size of the different distributions (Supporting Information Figures S2 and S3).

Effect of the Addition of "Free" Benzoic Acid on α-BA-PS Solutions. The purpose of adding "free" BA into toluene solutions of α-BA-PS is to increase the concentration of MAO-like species embedded within the micelles. Thus, various amounts of "free" BA, from 2 to 10 equivalents with respect to α-BA-PS, were tested. Two methods of BA addition were investigated. In a first method, free BA was added into previously prepared α-BA-PS solutions. In this case, the micellar organization and the size of the nanoparticles remain unchanged, suggesting that free BA is not able to penetrate the micellar aggregates (see Supporting Information Figure S4). In contrast, when free BA is initially added together with α-BA-PS in toluene, a dramatic size increase of the micellar aggregates was noted, from R_H = 195 nm to $R_H >$ 600 nm (see Figure 5).

The behavior of α-BA-PS solutions in toluene as a function of the concentration of additional BA molecules can be summarized as in Scheme 2. Table S1 (see Supporting Information) gathers the DLS data.

TEM Analysis of α-BA-PS in Toluene. To have a complementary description of the micellar morphology of α-BA-PS solutions, the samples were analyzed by transmission electronic microscopy (TEM). The TEM images were obtained from deposits of α-BA-PS solutions in toluene on the grid, followed by solvent evaporation. The morphology obtained from α-BA-PS (M_n = 5200 g/mol) solution at 6 mg/mL in toluene is presented in Figure 6. Two populations of spherical nanoparticles are observed: one of relatively broad distribution with an average diameter of 300 nm and another relatively narrow population of about 25 nm. Taking into account that the particles are generally flattened on the grid, these results are in good agreement with the DLS data ($R_H \sim$ 170 and 10.4 nm (±2.5%), see Figure 3).

Use of Self-Assembled α-BA-PS as Support for Tridentate Bis(imino)pyridinyliron/TMA Catalyst. *1. Addition of TMA onto α-BA-PS Solutions in Toluene.* The self-assembled nanostructures obtained from α-BA-PS were subsequently used as organic supports for the tridentate bis(imino)pyridinyl iron catalyst. To this end, TMA was added to α-BA-PS solutions and the reaction was carried out for 48 h at 60 °C (Supporting Information Scheme S1). The formation of MAO-like species was confirmed by ^{1}H NMR, as shown in Figure 7. The absence of signal attributed to free TMA at −0.38 ppm indicates the complete consumption of TMA while the presence of a new broad signal located from −0.8 to −0.2 ppm corresponds to the formation of $Me_2AlOAlMe_2$ species.

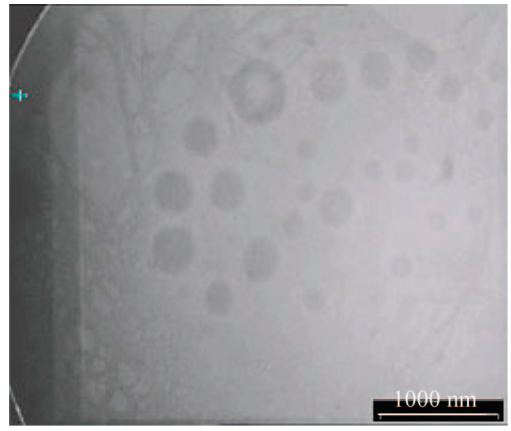

Figure 6. TEM pictures of α-BA-PS (M_n = 5600 g/mol) in toluene (c = 6 mg/mL) showing nanoparticles of different sizes.

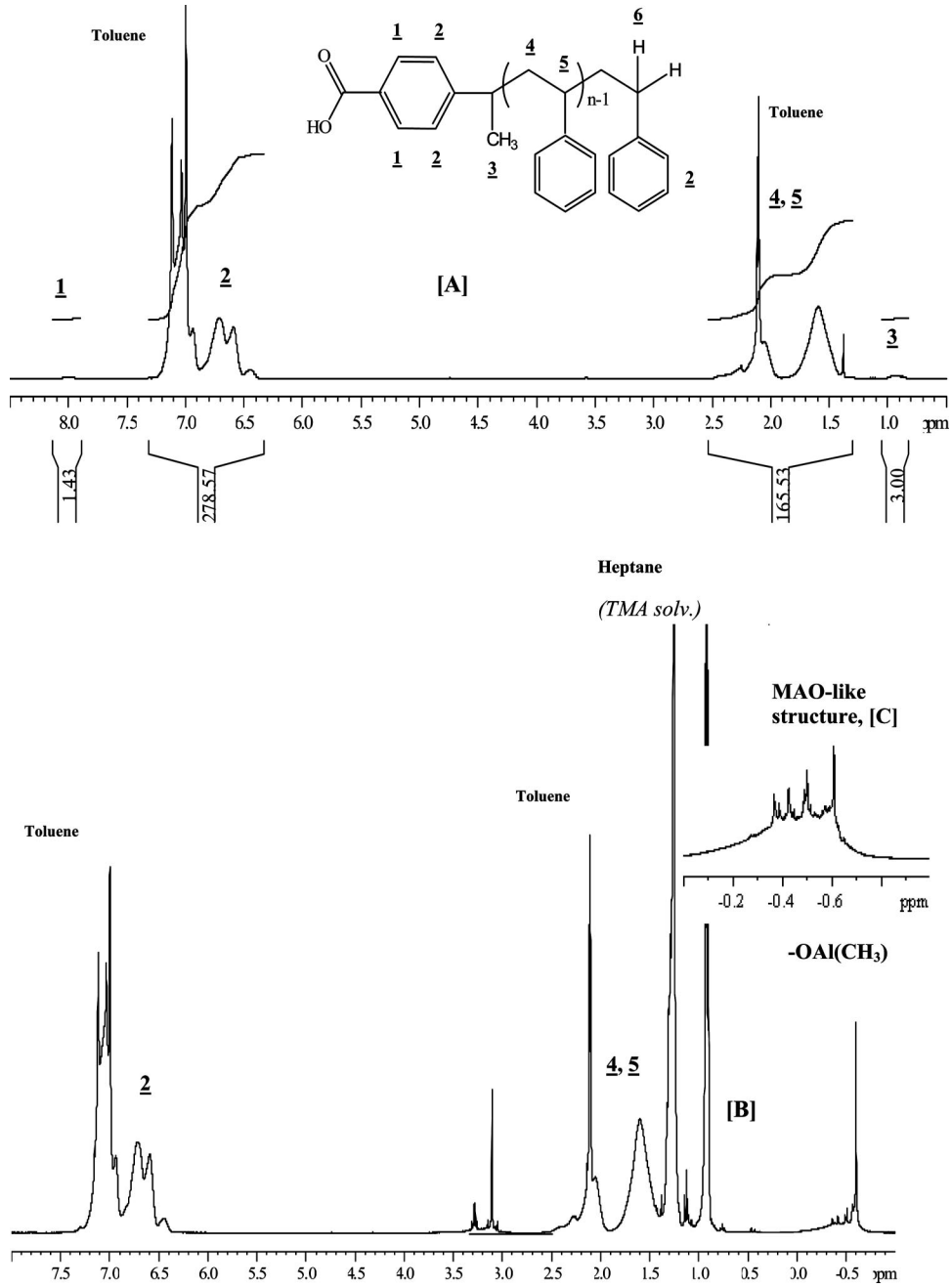

Figure 7. ^{1}H NMR spectra (400 MHz, toluene-d_8) of α-BA-PS before [A] and after addition of TMA at 60 °C: TMA/BA = 5 after 7 h [B] and after 60 h [C].

Table 2. Effect of TMA Addition on the Micellar Organization of α-BA-PS Solutions in Toluene in the Presence or Not of "Free" Benzoic Acid

entry	nature of the solution	$\bar{M}_{n,\alpha\text{-BA-PS}}$ (g/mol)	concn (mg/mL)	TMA/total BA	R_H before addition of TMA (nm)	R_H after addition of TMA (nm)
1	α-BA-PS in toluene	5200	30	5	260/101/2.5	947/101/18/2.8
2	α-BA-PS in toluene	5200	6	5	172/10.4/2.46	600/11.8/2.80
3	α-BA-PS in toluene	3600	18	3	250/14/2.20	412/5.75
4	BA/α-BA-PS = 2 in toluene	3600	18	3	460/14/2	1000/33
5	BA/α-BA-PS = 10 in toluene	3600	18	3	640/75.0/11.0/1.8	680/82.5/11.5/2.1

The effect of TMA addition onto the α-BA-PS self-assembly process in toluene was further investigated by DLS. Data are collected in Table 2. As also shown in Figure 8, the addition of TMA onto α-BA-PS solutions (M_n = 5200 g/mol, c = 30 mg/mL) leads to a limited change in the micelle diameter (R_H varies from (10.4 ± 0.26) nm to (11.8 ± 0.30) nm) but to a large increase of the size of the aggregates (from ~ 170−190 nm to more than 600 nm). Both NMR data and the increase of R_H values after addition of TMA indicate that the latter reacts with BA functions to form encapsulated MAO-like species.

As for α-BA-PS solutions containing free BA molecules, the size of micellar structures formed after addition of TMA was found to be impacted by the overall concentration of BA molecules added and trapped within the nanoparticles (entries 4 and 5, Table 2). A dramatic size increase of the aggregates is observed when TMA is added onto α-BA-PS

Table 3. Polymerization of Ethylene in the Presence of the Catalytic System Composed of α-BA-PS/TMA/MeDIP(2,6-iPrPh)$_2$FeCl$_2$[a]

entry[b]	$M_{n,\alpha\text{-BA-PS}}$	[α-BA-PS] (mg/mL)	TMA/BA$_{total}$[c]	Al/Fe	activity (kg PE/ (mol Fe·h·bar))	density (g/L)	M_w[d] (kg/mol)	D[d]
1	6100	6	5	300	815	320	–	–
2	6100	6	5	500	1100	300	1160	bimodal
3	6100	30	5	500	150	n.d.	–	–
4	5200	6	3	300	2100	370	–	–
5	5200	30	3	300	2340	450	–	–
6	5200	40	3	300	425	n.d.	545	bimodal
7	5200	57	5	300	2590	380	440	bimodal
8	3600	20	5	300	1420	400	510	27
9	3600	20	3	300	540	n.d.	365	12

[a] Experimental conditions: toluene, 45 mL; reaction time = 1 h; T = 30 °C; $P_{ethylene}$ = 1 atm. [b] Polymers have been stirred for 6 h at 25 °C before addition of TMA. [c] Reaction time before polymerization = 48 h at 60 °C under stirring. [d] Determined by SEC (1, 2, 4-trichlorobenzene at 150 °C).

Table 4. Polymerization of Ethylene in the Presence of the Catalytic System Composed of α-BA-PS + "Free" Benzoic Acid/TMA/MeDIP(2,6-iPrPh)$_2$FeCl$_2$[a]

entry[b]	quantity of BA added[c]	[α-BA-PS] (mg/mL)	TMA/BA$_{total}$ [d]	Al/Fe	activity (kg PE/ (mol Fe·h·bar))	density (g/L)	$\bar{M}_w$[e] (kg/mol)	D[e]
1[f]	10	18	3	200	0	–	–	–
				300	1425	270	286	2.0
				400	1400	n.d.	–	–
				500	1540	290	215	2.3
2[f]	10	50	3	400	1275	275	280	2.2
3[f]	5	18	3	300	900	380	280	2.1
				500	1115	270	252	2.0
4[f]	2	18	3	400	675	220	377	2.5

[a] Experimental conditions: toluene, 45 mL; reaction time = 1 h; T = 30 °C; $P_{ethylene}$ = 1 atm. [b] Polymers associated with "free" benzoic acid have been stirred for 6 h at 25 °C before addition of TMA. [c] Quantity of benzoic acid added as a function of the quantity of benzoic acid present in the functionalized polystyrenes. [d] Reaction time before polymerization = 48 h at 60 °C under stirring. [e] Determined by SEC (1,2,4-trichlorobenzène at 150 °C). [f] BA-PS-H: M_n = 3600 g/mol.

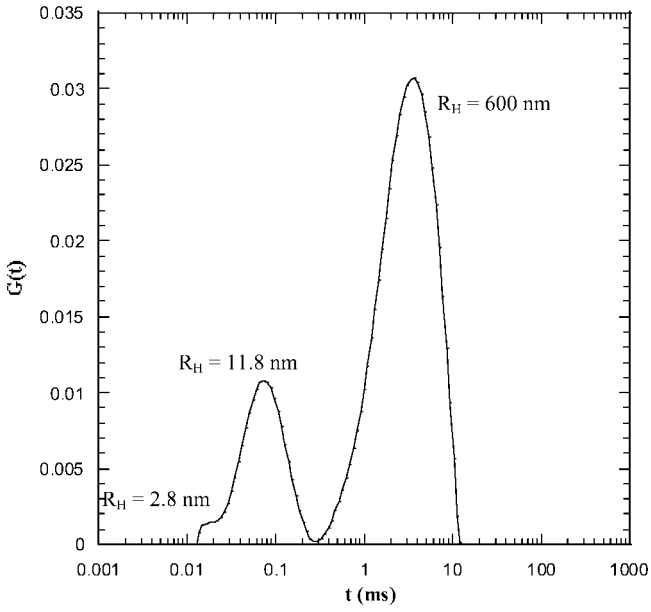

Figure 8. Relaxation times of α-BA-PS (M_n = 5200 g/mol) in toluene at 6 mg/mL in the presence of TMA (TMA/BA = 5) at 25 °C (θ = 90°).

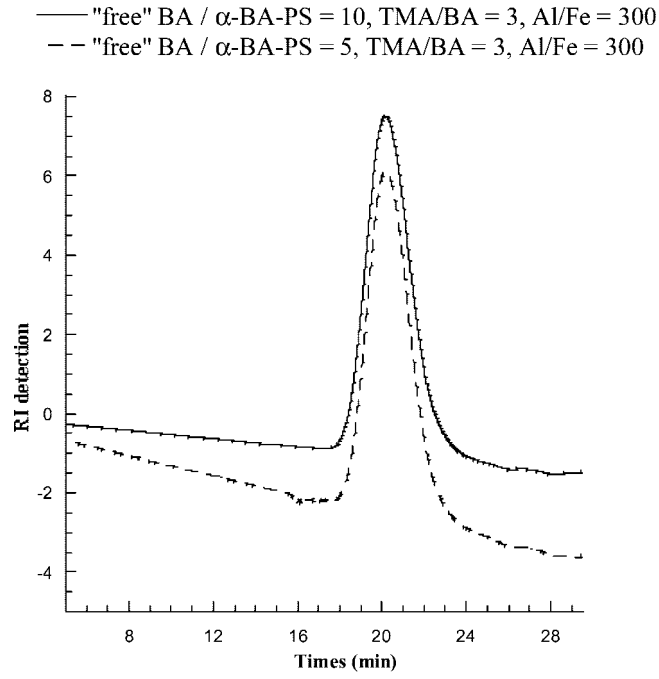

Figure 9. SEC traces of PE prepared in the presence of α-BA-PS (M_n = 3600 g/mol) particles with free BA in toluene ([α-BA-PS = 18 mg/mL]), TMA, and the iron catalyst (eEntries 1 and 3, Table 4).

solutions containing a low amount of BA molecules (entry 4), as already observed in the absence of free BA molecule. It can be expected that aluminic species formed in this case are not fully trapped within the core of the micelles and rather contribute to the micellar aggregation through the formation of aluminic bridges. In contrast, for high BA/α-BA-PS ratios (entry 5), only a limited change in the size of the aggregates is observed upon addition of TMA. In the latter case, it is likely that TMA better diffuses and is trapped more easily into the nanoparticles (aggregates).

Despite the fact that the so-formed 'activated' micelles were probably not all at the thermodynamic equilibrium, they were used as such as supports for MeDIP(2,6-iPrPh)$_2$FeCl$_2$ toward ethylene polymerization. The effect of additional free BA and TMA/BA ratio on catalytic activity as well as on the polyethylene (PE) molar mass and morphology was investigated.

2. Ethylene Polymerization in the Presence of 'Activated Micelles' without Free BA. MeDIP(2,6-iPrPh)$_2$FeCl$_2$ was added onto toluene solutions containing α-BA-PS micellar structures embedding MAO-like species in a glass reactor, then ethylene was introduced under 1 bar at 30 °C for one hour. The polymerization data are collected in Table 3.

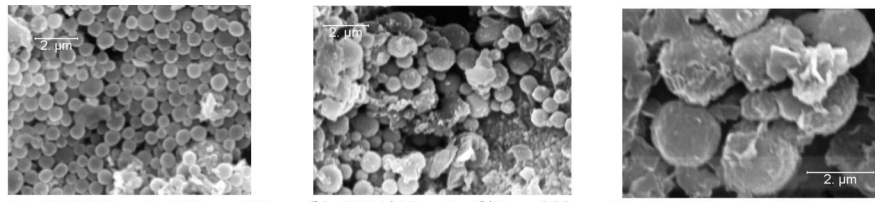

(a): TMA/AB = 3, Al/Fe = 300 $\overline{M}_{n\ \alpha\text{-BA-PS}}$ *= 3600 g/mol*

(b): TMA/AB = 5, Al/Fe = 300 $\overline{M}_{n\ \alpha\text{-BA-PS}}$ *= 5200 g/mol*

(c): TMA/AB = 5, Al/Fe = 500, $\overline{M}_{n\ \alpha\text{-BA-PS}}$ *= 6100 g/mol*

Figure 10. SEM pictures of PE particles prepared in the presence of α-BA-PS/TMA/MeDIP(2,6-iPrPh)$_2$FeCl$_2$.

Under these conditions, catalytic activities varied from 150 to nearly 2 600 kg PE/(mol Fe·h·bar). These values are higher than those obtained in the presence of nanogel supports bearing peripheral benzoic acid end groups (activity = 490 kg PE/(mol Fe·h·bar) for TMA/BA = 3 and Al/Fe = 300)[27] and, in some cases, can exceed values obtained with commercial MAO (activity = 1260 kg PE/(mol Fe·h·bar) for MAO/Fe = 455).[14] Moreover, high molar mass PEs are obtained in the presence of micellar supports. However, the dispersity (D) of the resulting PEs is somewhat broad and varies with the molar mass of α-BA-PS. PEs obtained in the presence of α-BA-PS supports with M_n = 6100 g/mol and 5200 g/mol show a bimodal distribution, suggesting that TMA is not entirely trapped within the micelles and that free TMA reacts with the iron catalyst under homogeneous conditions. In contrast, α-BA-PS with M_n =3600 g/mol leads to a monomodal although broad molar mass distribution (Supporting Information Figure S5). This result strongly supports that the transfer reaction to TMA is significantly reduced, using the micellar supports generated from α-BA-PS of the lowest molar mass. This can be logically attributed to the presence of a limited amount of "free" TMA and thus to the effective formation of more stable nanoparticles/MAO-like species assemblies when using the lower molar mass α-BA-PS.

3. Ethylene Polymerization in the Presence of 'Activated Micelles' Containing Free BA. As shown in Table 4, the catalytic activity increases with the Al/Fe ratio as well as with the amount of BA trapped within the micelles. More interestingly is the monomodal molar mass distribution ($D \sim 2$) of PEs obtained in such conditions, as illustrated in Figure 9. This clearly indicates that additional BA enables a complete consumption of free TMA thus limiting dramatically transfer reactions to TMA, as commonly observed with iron based catalysts.[35,36]

4. Polyethylene Morphology. As indicated in Tables 3 and 4, PEs with high bulk densities (between 220 and 460 g/L) were obtained in agreement with a supported polymerization. This was further confirmed after examination of the morphology of PE samples by optical microscopy and SEM analyses. PEs prepared with α-BA-PS without additional "free" BA show spherical-type morphology (Figure 10). Very homogeneous PE particles are obtained in the presence of the more stable micelles arising from the low molar mass α-BA-PS. In addition, the diameter of the PE beads increases significantly with the molar mass of α-BA-PS from about 0.2 to 2 μm, the higher value being comparable with previous results obtained from self-assembled PS-b-P(4-VBA) block copolymers used as micellar supports.[28]

A very sensitive change in the PEs particle size is observed with micelles containing additional "free" BA (free BA/α-BA-PS > 5).

Well-defined spherical beads with an average diameter of 2 mm are formed, which is unusual in a slurry process. Increasing the amount of free BA and therefore the amount of MAO-like species also improves the beads size distribution and morphology (Figure 11). This can be related to the size increase of the micelles and aggregates, which facilitates the diffusion of iron catalyst and of the monomer within the nanoparticles.

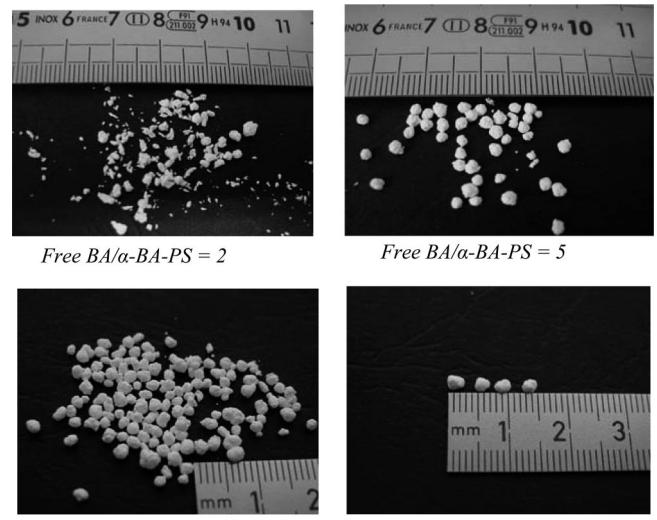

Free BA/α-BA-PS = 2 *Free BA/α-BA-PS = 5*

Free BA/α-BA-PS = 10

Figure 11. Pictures of PE particles prepared in the presence of α-BA-PS (M_n = 3600 g/mol) associated with benzoic acid molecules ([α-BA-PS] = 18 mg/mL), TMA (TMA/BA$_{total}$ = 3), and the iron catalyst.

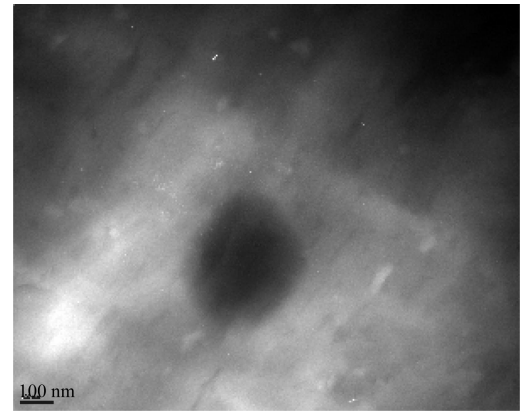

Figure 12. TEM image of a cross-section of millimetric PE beads showing embedded PS support. The central black spot corresponds to stained PS while the surrounding white zone is constituted of PE chains.

To further confirm the role of the amphiphilic PS-based support, ultrathin cryo-cuts of the PE beads were prepared, and the PS phase was selectively stained with RuO_4 before analysis by TEM. The TEM images clearly show the presence of PS residue inside the PE beads, confirming the role of the support during the polymerization (Figure 12). The size of the supports observed on TEM images (diameter ~ 300 nm) can be attributed to micellar aggregates, which suggests that PE beads would be formed around them.

Conclusion

We report, for the first time, the use of amphiphilic polystyrene chains, i.e., benzoic acid end-functionalized polystyrene (α-BA-PS), as elementary building blocks that can self-assemble in toluene leading to organic nanoreactors for supported ethylene polymerization. TMA could indeed diffuse into the micellar nanostructures and react with BA moieties of the PS chain-ends thus forming MAO-like aluminic species embedded in the micellar cores. Free BA molecules could be possibly added onto the micellar solutions in order to increase the concentration of MAO-like species. When used as supports for $MeDIP(2,6\text{-}iPrPh)_2FeCl_2$, these activated micelles enable the production of unprecedented well-defined millimetric PE beads with good catalytic activity.[37] This concept is now extended to the preparation of other supported polymerization catalysts and to the polymerization of other vinyl monomers in different media.

Acknowledgment. Financial support from French Ministry of Research and Education, Centre National de la Recherche Scientifique, and Institut Universitaire de France is acknowledged. The authors are grateful to O. Boyron (LCPP-Lyon) for SEC analyses and to R. C. Hiorns for helpful discussions.

Supporting Information Available: DLS data on PS and BA, and the reaction between TMA and BA in homogeneous conditions. This material is available free of charge via the Internet at http://pubs.acs.org.

References and Notes

(1) Fink, G.; Steinmetz, B.; Zechlin, J.; Przybyla, C.; Tesche, B. *Chem. Rev.* **2000**, *100*, 1377.
(2) Hlatky, G. G. *Chem. Rev.* **2000**, *100*, 1347.
(3) Ferrero, M. A.; Chiovetta, M. G. *Polym. Eng. Sci.* **1987**, *19*, 1436.
(4) Severn, J. S.; Chadwick, J. C.; Duchateau, R.; Friederichs, N. *Chem. Rev.* **2005**, *105*, 4073.
(5) Nishida, H.; Uozumi, T.; Arai, T.; Soga, K. *Macromol. Rapid Commun.* **1995**, *16*, 821.
(6) Kitagawa, T.; Uozumi, T.; Soga, K.; Takata, T. *Polymer* **1997**, *38*, 615.
(7) Hong, S. C.; Ban, H. T.; Kishi, N.; Jin, J.; Uozumi, T.; Soga, K. *Macromol. Chem. Phys.* **1998**, *199*, 1393.
(8) Barrett, A. G. M.; de Miguel, Y. R. *Chem. Commun.* **1998**, *2079*000.
(9) Hong, S. C.; Rief, U.; Kristen, M. O. *Macromol. Rapid Commun.* **2001**, *22*, 1447.
(10) Wang, W.; Wang, L.; Wang, J.; Wang, J.; Ma, Z. *J. Polym. Sci. Part A: Polym. Chem.* **2005**, *43*, 2650.
(11) Koch, M.; Falcou, A.; Nenov, N.; Klapper, M.; Müllen, K. *Macromol. Rapid Commun.* **2001**, *22*, 1455.
(12) Jang, Y.-J.; Nenov, N.; Klapper, M.; Müllen, K. *Polym. Bull.* **2003**, *50*, 343.
(13) Jang, Y.-J.; Nenov, N.; Klapper, M.; Müllen, K. *Polym. Bull.* **2003**, *50*, 351.
(14) Bouilhac, C.; Cloutet, E.; Cramail, H.; Deffieux, A.; Taton, D. *Macromol. Rapid Commun.* **2005**, *26*, 1619.
(15) Bartke, M.; Oksman, M.; Mustonen, M.; Denifl, P. *Macromol. Mater. Eng.* **2005**, *290*, 250.
(16) Denifl, P.; Van Praet, E.; Bartke, M.; Oksman, M.; Mustonen, M.; Garoff, T.; Pesonen, K. PCT Int. Appl. 03/051934. *Chem. Abstr.* **2003**, *139*, 53479.
(17) Nenov, S.; Clark, C. G.; Klapper, M.; Müllen, K. *Macromol. Chem. Phys.* **2007**, *208*, 1362.
(18) Klapper, M.; Nenov, S.; Diesing, T.; Müllen, K. *Macromol. Symp.* **2007**, *260*, 90.
(19) Mecking, S.; Monteil, V.; Huber, J.; Kolb, L.; Wehrmann, P. *Macromol. Symp.* **2006**, *236*, 117.
(20) Mecking, S. *Colloid Polym. Sci.* **2007**, *285*, 605.
(21) Göttker-Schnetmann, I.; Korthals, B.; Mecking, S. *J. Am. Chem. Soc.* **2006**, *128*, 7708.
(22) Kissin, Y. V. *Macromolecules* **2003**, *36*, 7413.
(23) Busico, V.; Cipullo, R.; Cutillo, F.; Friederichs, N.; Ronca, S.; Wang, B. *J. Am. Chem. Soc.* **2003**, *125*, 12402.
(24) Dalet, T.; Cramail, H.; Deffieux, A. *Macromol. Symp.* **2006**, *231*, 110.
(25) Dalet, T.; Cramail, H.; Deffieux, A. *Macromol. Chem. Phys.* **2004**, *205*, 1394.
(26) Bouilhac, C.; Cramail, H.; Cloutet, E.; Deffieux, A.; Taton, D. *J. Polym. Sci. Part A: Polym. Chem.* **2006**, *44*, 6997.
(27) Bouilhac, C.; Cloutet, E.; Deffieux, A.; Taton, D.; Cramail, H. *Macromol. Chem. Phys.* **2007**, *208*, 1349.
(28) Bouilhac, C.; Cloutet, E.; Taton, D.; Deffieux, A.; Borsali, R.; Cramail, H. *J. Polym. Sci. Part A: Polym. Chem.* (submitted).
(29) Small, B. L.; Brookhart, M.; Bennett, A. M. A. *J. Am. Chem. Soc.* **1998**, *120*, 4049.
(30) Provencher, S. W. *Comput. Phys. Commun.* **1982**, *27*, 213.
(31) Malz, H.; Komber, H.; Voigt, D.; Hopfe, I.; Pionteck, J. *Macromol. Chem. Phys.* **1999**, *200*, 642.
(32) Zhang, X.; Matyjaszewski, K. *Macromolecules* **1999**, *32*, 7349.
(33) Voulgaris, D.; Tsitsilianis, C.; Grayer, V.; Esselink, F. J.; Hadziioannou, G. *Polymer* **1999**, *40*, 5879.
(34) Balsara, N. P.; Tirrell, M.; Lodge, T. P. *Macromolecules* **1991**, *24*, 1975.
(35) Kumar, K. R.; Sivaram, S. *Macromol. Chem. Phys.* **2000**, *201*, 1513.
(36) Wang, Q.; Yang, H.; Fan, Z. *Macromol. Rapid Commun.* **2002**, *23*, 639.
(37) Cramail, H.; Bouilhac, C.; Cloutet, E.; Deffieux, A.; Taton, D. FR N°0704328 (June 0702007).

MA8016772